



## Influence of Solvents on the Structural and Electrochemical Properties of $\text{Li}[\text{Li}_{0.2}\text{Ni}_{0.1}\text{Co}_{0.2}\text{Mn}_{0.5}]\text{O}_2$ Prepared by a Solvothermal Reaction Method

Chi-Hoon Song, A. Manuel Stephan,<sup>a</sup> Soo Kyung Jeong, Yun Ju Hwang, Ae Rhan Kim, and Kee Suk Nahm<sup>z</sup>

School of Chemical Engineering and Technology, Chonbuk National University, Chonju 561-756, South Korea

Solid solutions of  $\text{Li}[\text{Li}_{0.2}\text{Ni}_{0.1}\text{Co}_{0.2}\text{Mn}_{0.5}]\text{O}_2$  were prepared by solvothermal reaction with three different solvents, namely, methanol, ethanol, and 1-propanol. The prepared compounds were subjected to X-ray diffraction (XRD), Raman, Fourier transform infrared, and charge-discharge studies. XRD studies revealed that the prepared compounds are of layered structure with space group  $R\bar{3}m$ . The sample which was prepared using 1-propanol as solvent delivered the highest discharge capacity of 205 mAh/g. The electrochemical and structural properties of the prepared compounds are influenced by the physical properties of the solvents. © 2006 The Electrochemical Society. [DOI: 10.1149/1.2149301] All rights reserved.

Manuscript submitted August 5, 2005; revised manuscript received October 18, 2005. Available electronically January 4, 2006.

Layered manganese oxides are found to be attractive cathode materials for lithium batteries because of low cost, nontoxicity, high voltage, and capacity. However, the layered  $\text{LiMnO}_2$  undergoes structural transformation (to spinel) upon prolonged cycling. In order to circumvent this problem, many researchers have studied the solid solutions between  $\text{LiMO}_2$  ( $M = \text{Mn}, \text{Ni}, \text{Co}, \text{etc.}$ ) and  $\text{Li}[\text{Li}_{1/3}\text{Mn}_{2/3}]\text{O}_2$  to stabilize the layered structure.<sup>1,2</sup>

Generally, solid solutions are prepared by the sol-gel method, whose advantages are high reactivity of the mixture at lower heat-treatment of materials, good stoichiometry, and smaller particles of uniform size. Synthesis of cathode materials by a conventional solid-state reaction method involves high temperature, long and repeated heat-treatment, and extended grinding. In addition, this method has also some disadvantages such as inhomogeneity, irregular morphology, larger particle size, broad particle size distribution, and poor stoichiometry.<sup>1-5</sup> In order to enhance the solid phase diffusivity, many researchers have attempted to synthesize solid solutions by the addition of solvents in the precursors.<sup>6-14</sup> Guo et al.<sup>6</sup> reported the synthesis of the material,  $\text{LiCr}_x\text{Mn}_{1-x}\text{O}_2$ , by solid-state reaction with ethanol as solvent, which delivered a discharge capacity of 160 mAh  $\text{g}^{-1}$  with excellent cyclability. Recently, in a similar study, Kim and Chung<sup>7,8</sup> prepared layered  $\text{Li}[\text{Ni}_{1/3}\text{Co}_{1/3}\text{Mn}_{1/3}]\text{O}_2$  and  $\text{Li}[\text{Ni}, \text{Co}, \text{Mn}]\text{O}_2$  with ethanol as solvent. These materials are found to be stable without any capacity fading. Pistoia and Rosati<sup>9</sup> also synthesized spinel  $\text{LiMn}_2\text{O}_4$  by solid-state reaction with alcohol and cyclohexane as dispersion agents in which the authors obtained the materials of smaller size with increased surface area, resulting in excellent electrochemical properties. Xiao et al.<sup>10</sup> compared the electrochemical properties of  $\text{LiMn}_x\text{Cr}_{1-x}\text{O}_2$  compound prepared by solid-state reaction and rheological routes. The authors found that the material obtained through the rheological method was suitable when electrochemical properties are concerned. Recently, Sun et al.<sup>11</sup> reported that the layered  $\text{Li}[\text{Ni}_{0.5-x}\text{Co}_{2x}\text{Mn}_{0.5-x}]\text{O}_2$  structure could be achieved by solid-state reaction combined with high-energy ballmilling. According to the authors, the process of simple ballmilling facilitates the formation of the compound with good stoichiometry and also delivered the discharge capacity of 142–185 mAh/g with excellent cyclability. The above literature studies<sup>5-10</sup> revealed that the materials prepared using solvents offer a stable structure and show excellent electrochemical properties. So far to the best of our knowledge, not much attention has been devoted to the synthesis of lithium manganese oxide materials with different solvents. In the present study,  $\text{Li}[\text{Li}_{0.2}\text{Ni}_{0.1}\text{Co}_{0.2}\text{Mn}_{0.5}]\text{O}_2$

solid solution was synthesized using a solvothermal reaction method with different alcohols of various alkyl group lengths, namely, methanol, ethanol, or 1-propanol as solvent. Also, we have explored the reaction mechanism that takes place during the synthesis process and the structural and electrochemical properties of the prepared materials are discussed.

### Experimental

$\text{Li}[\text{Li}_{0.2}\text{Ni}_{0.1}\text{Co}_{0.2}\text{Mn}_{0.5}]\text{O}_2$  precursors were synthesized from starting materials of  $\text{LiOH}\cdot\text{H}_2\text{O}$  (Aldrich),  $\text{Ni}(\text{OH})_2$  (Kita Chemical),  $\text{Co}(\text{OH})_2$  (Aldrich), and  $\text{MnOOH}$  (Junsei) powders by a solvothermal reaction method with variable solvents (methanol, ethanol, 1-propanol). The starting materials were charged into a zirconia vial in molar ratio of  $\text{Li}/\text{Ni}/\text{Co}/\text{Mn} = 6/5/1/10:1/5/1/2$  with two zirconia balls of 12.7 mm and six zirconia balls of 7 mm diameter and with various solvents (1.0  $\text{cm}^3/\text{g}$  of solid). The ground mixtures were obtained with a ball miller (Fritsch; Planetary Mono Mill-Pulverisette 6) for 4 h. To evaporate solvents, the mixed material was dried at 100°C for 24 h in a vacuum oven. The ground mixture materials were preheated at 600°C for 5 h in air and were ground in an agate mortar. The ground mixture materials were calcinated at 960°C for 10 h in air. Thus, the synthesized samples were named A, B, C, and D without solvent, with methanol, ethanol, and 1-propanol, respectively. In order to avoid the loss of lithium due to evaporation, an excess of lithium up to 10% was added. The Li, Co, Mn, and Ni contents in the resulting materials was analyzed using an inductively coupled plasma/atomic emission spectrometer (ICP/AES, Kontron-S 35). The powder X-ray diffraction (XRD, D/Max 2500, Rigaku) measurement using  $\text{Cu K}\alpha$  radiation was employed to characterize the crystalline phase of the synthesized materials. XRD measurements were carried out in the  $2\theta$  range of 10–80° with a scan speed of 4°/min and sampling width of 0.02°.

Rietveld refinement was performed on the XRD profiles to identify the variation of unit cell constant, and the data were collected by a Rietveld Program (Fullprof 2000, LLB). Although the Rietveld analysis is a powerful technique to find the ion occupancy of lithium and manganese, in the present study we have used the same to find the lattice parameter values. Also, the crystal structure of synthesized material was confirmed by micro-Raman spectrometer (RS spectra, RS 100, Reinshaw) with holographic gratings. The laser light source was the 514-nm line radiation from a Spectra-Physics 2020 argon-ion laser.

Fourier transform infrared (FTIR) spectroscopy absorption spectra were recorded using an FTIR MB 100, ABB Bomem model, at room temperature in the spectral range 4000–400  $\text{cm}^{-1}$ . The spectrometer was equipped with a 3.5- $\mu\text{m}$ -thick beam splitter, a global source and a DTGS/PE far-infrared detector. The sample was ground

<sup>a</sup> Present address: Central Electrochemical Research Institute, Karaikudi 630 006, India.

<sup>z</sup> E-mail: nahmks@chonbuk.ac.kr

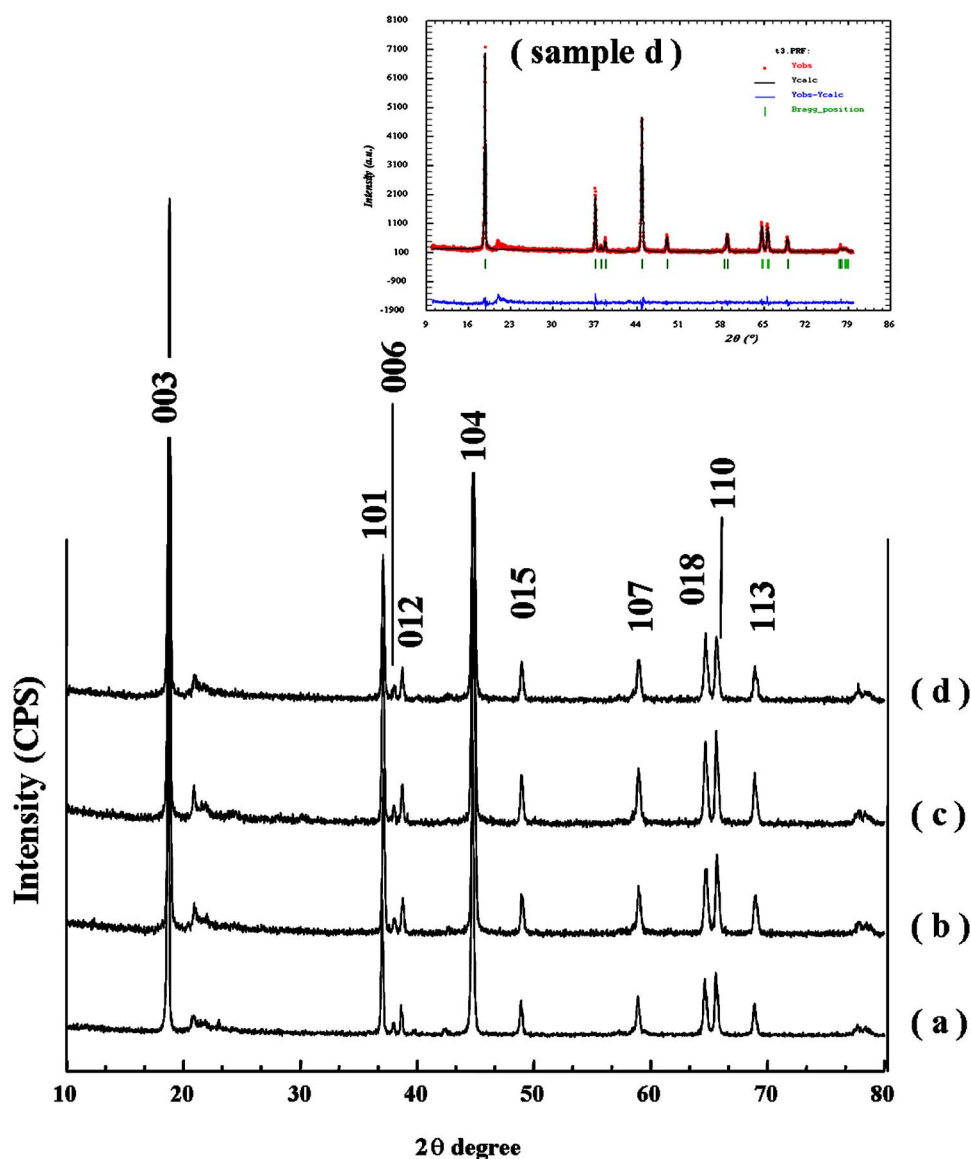


**Figure 1.** X-ray patterns of  $\text{Li}[\text{Li}_{1/5}\text{Ni}_{1/10}\text{Co}_{1/5}\text{Mn}_{1/2}]\text{O}_2$  materials with variable solvents (a) without solvent, (b) with methanol, (c) with ethanol, and (d) with 1-propanol.

with KBr in the form of fine powder and was pelletized. The data were collected after 256 scans with a spectral resolution of  $2\text{ cm}^{-1}$ .

The electrochemical characterization was carried out using a 2032-type coin cell (Hosen). For fabrication of the cathode electrode, 20 mg of  $\text{Li}[\text{Li}_{0.2}\text{Ni}_{0.1}\text{Co}_{0.2}\text{Mn}_{0.5}]\text{O}_2$  compounds were mixed with 12 mg of conductive binder (8 mg of “Teflonized” acetylene black and 4 mg of graphite). The mixture was pressed on  $2.0\text{-cm}^2$  stainless steel mesh used as the current collector and dried at  $100^\circ\text{C}$  for 10 h in a vacuum oven. The cells were composed of the cathode and the lithium foil (Cyprus Foote Mineral) anode, separated by porous polypropylene film separator (Celgard 3401). The electrolyte was 1 M  $\text{LiPF}_6$ —ethylene carbonate (EC)/dimethyl carbonate (DMC) with a 1:2 volume ratio (Merk). The cells were assembled in an argon-filled dry box and tested at  $30^\circ\text{C}$ . The cutoff voltages were 2.5 and 4.5 V, with a current density of  $0.4\text{ mA/cm}^2$ .

### Results and Discussion

From the ICP/AES analysis the composition of the compound was found to be  $\text{Li}_{1.20}\text{Ni}_{0.1}\text{Co}_{0.201}\text{Mn}_{0.5}\text{O}_2$ . Figure 1a-d shows the XRD patterns of  $\text{Li}[\text{Li}_{0.2}\text{Ni}_{0.1}\text{Co}_{0.2}\text{Mn}_{0.5}]\text{O}_2$  prepared by solvothermal reaction method at  $960^\circ\text{C}$  without solvent, with methanol, ethanol, or 1-propanol as solvents, respectively. A typical Reitveld fit plot is also shown for better understanding. All diffraction peaks are

indexed to a hexagonal  $\alpha\text{-NaFeO}_2$  structure (S.G:  $R\bar{3}m$ , 166) except the peaks between  $21$  and  $25^\circ$ . The broad XRD peaks between  $21$  and  $25^\circ$  are a superstructure peak, resulting from superlattice ordering of Li, Ni, Co, and Mn atoms on the transition-metal layers.<sup>12</sup> The main peaks (003) and (104) appear at  $2\theta = 18$  and  $45^\circ$ , respectively. The intensity ratios of (003)/(104) peaks for all the samples are above 1.39. Therefore, as-prepared samples represent a hexagonal  $\alpha\text{-NaFeO}_2$  structure. The clear splitting of the lines assigned to Miller indices (006), (102), and (108), (110) is a characteristic feature of a typical layered structure. According to Morales et al.,<sup>13</sup> the (003) peak occurs from the diffraction of the layered rock-salt structure ( $R\bar{3}m$ ), whereas the (104) peak occurs from both the diffraction of layered and cubic rock-salt structures. Some researchers reported<sup>11,12</sup> that layered cathode materials show good electrochemical properties when the intensity ratio of (003) and (104) peaks is higher than 1.2 and when the (101), (006) and (108), (110) peaks are clearly split.<sup>12</sup> In the present study, a clear split has been observed in the above said peaks, which confirms the formation of the compound.

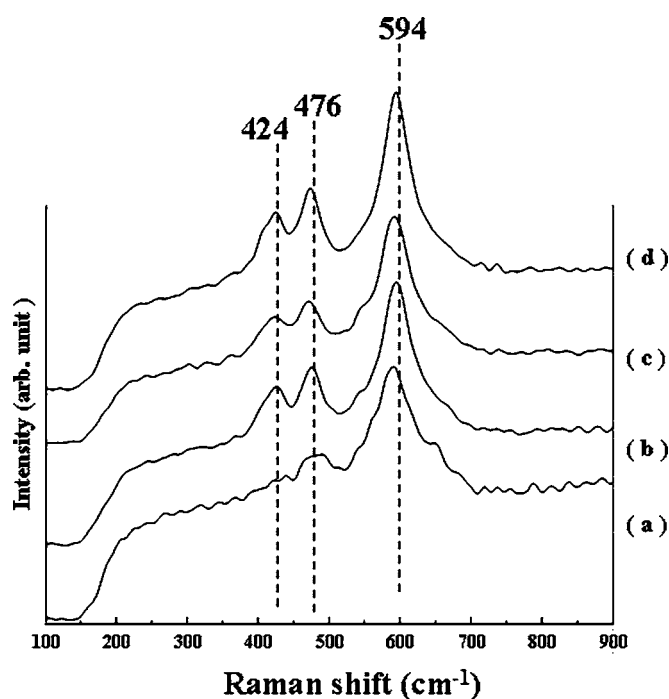
Table I depicts the lattice parameters determined by Rietveld refinement based on hexagonal  $\alpha\text{-NaFeO}_2$  for  $\text{Li}[\text{Li}_{0.2}\text{Ni}_{0.1}\text{Co}_{0.2}\text{Mn}_{0.5}]\text{O}_2$  samples prepared with different solvents.

**Table I.** The lattice parameters of  $\text{Li}[\text{Li}_{0.2}\text{Ni}_{0.1}\text{Co}_{0.2}\text{Mn}_{0.5}]\text{O}_2$  prepared by solvothermal reaction method.

Sample	Solvents	Lattice parameter (Å)			R-factors (%)	
		<i>a</i>	<i>c</i>	<i>c/a</i>	<i>R<sub>p</sub></i>	<i>R<sub>w</sub></i>
A	No	2.843	14.209	4.998	15.9	19.2
B	Methanol	2.845	14.224	4.999	13.4	15.6
C	Ethanol	2.845	14.218	4.998	13.2	15.3
D	1-Propanol	2.845	14.219	4.998	13.5	16.6

As shown in Table I, the *c/a* ratio of the prepared samples is more than 4.9, which means that all the samples are similar in structure. According to Bruce et al.,<sup>14</sup> the *c/a* ratio of 4.9 indicates the rhombohedral cubic structure, and for the hexagonal structure it should be more than 4.9. More interestingly, in the present study all the samples show the *c/a* ratios between 4.998 and 4.999, irrespective of the solvent used. These results are in accordance with Julien et al.,<sup>15</sup> in which the authors reported the electrochemical properties of layered  $\text{LiNi}_{0.3}\text{Co}_{0.7}\text{O}_2$ . The intensity of the superstructure peak of sample A, which was prepared without solvent, is lower than that of samples B, C, and D prepared with solvents. Shin et al.<sup>16</sup> observed that the intensity of the superstructure peak increases with the increase of lithium content. In the present study an increase in intensity has been observed for samples B, C, and D prepared with solvents. Thus, it can be believed that more and more Li ions are inserted into the transition metal layers for the solvent-added compounds. These results confirm the formation of a hexagonal  $\alpha\text{-NaFeO}_2$  structure with  $\text{Li}_2\text{MnO}_3$  character of the synthesized  $\text{Li}[\text{Li}_{0.2}\text{Ni}_{0.1}\text{Co}_{0.2}\text{Mn}_{0.5}]\text{O}_2$  compound.<sup>3,4</sup>

Figure 2a-d shows Raman scattering spectra of synthesized samples without (Fig. 2a) and with (Fig. 2b-d) different solvents, respectively. The Raman-active modes for  $\text{LiMO}_2$  are located in the range 400 and 650  $\text{cm}^{-1}$ . The Raman-active modes of synthesized samples are recorded at 424, 476, and 594  $\text{cm}^{-1}$ , although with some differences in the intensities of peaks. The Raman spectra

**Figure 2.** Raman spectra of  $\text{Li}[\text{Li}_{0.2}\text{Ni}_{0.1}\text{Co}_{0.2}\text{Mn}_{0.5}]\text{O}_2$  with variable solvents (a) without solvent, (b) with methanol, (c) with ethanol, and (d) with 1-propanol.

agree well with the factor group analysis of the  $R\bar{3}m$  symmetry.<sup>17</sup> The peaks at 476 and 594  $\text{cm}^{-1}$  are assigned to the Raman-active species  $E_g$  and  $A_{1g}$  modes, respectively.<sup>18</sup> Generally, Raman bands are related to motion involving M–O stretching and O–M–O bending, as the contribution to the Raman modes are only from the motion of oxygen atoms. The  $A_{1g}$  mode has the greater oscillation strength and exhibits intensity twice that of the  $E_g$  mode.<sup>18,19</sup> The peaks at 424  $\text{cm}^{-1}$  of samples B, C, and D are related to  $\text{Li}_2\text{MnO}_3$  superlattice ordering. These results are in accordance with our XRD results of Fig. 1, in which all samples show a peak at 21°, indicating a superstructure peak related to  $\text{Li}_2\text{MnO}_3$ . According to Sun et al.<sup>3</sup> and Dahn et al.,<sup>4</sup> the peaks between 21 and 25° arise due to the superlattice ordering of Li, Ni, Mn, and Co in the 3a site, indicating a layered structure with  $\text{Li}_2\text{MnO}_3$  character. As observed in the XRD, the intensity of the peak for sample A is lower than that of sample B, C, and D. Similarly, the intensity of the peak observed at 424  $\text{cm}^{-1}$  for sample A is lower than that of other samples in the Raman spectra, which further substantiates that the characteristics of the samples prepared without solvent are entirely different from those of the sample prepared with solvent.

Figure 3a-d shows the charge–discharge curves of  $\text{Li}/\text{LiPF}_6\text{-EC/DMC}$  (1:2 by vol)/ $\text{Li}[\text{Li}_{0.2}\text{Ni}_{0.1}\text{Co}_{0.2}\text{Mn}_{0.5}]\text{O}_2$  cells cycled at 30°C for the cathode materials prepared with different solvents. All samples show a monotonic discharge curve with one step, which is a characteristic feature of typical layered structure. The solvents used during the synthesis process play an important role in the electrochemical properties of the compound. The irreversible capacity for samples A, B, C, and D are found to be 46, 90, 100, and 89 mAh/g, respectively, during the first cycling. The irreversible capacity due to oxygen loss<sup>4,20</sup> and extraction of Li ion on transition metal layers<sup>21</sup> is more for the samples prepared with solvents than that of the samples prepared without solvent, and the length of the irreversible capacity for sample A is shorter than that of other samples.

Figure 4a-d shows the cycle number vs discharge capacity profile of the fabricated  $\text{Li}/\text{LiPF}_6\text{-EC/DMC}$  (1:2 by vol)/ $\text{Li}[\text{Li}_{0.2}\text{Ni}_{0.1}\text{Co}_{0.2}\text{Mn}_{0.5}]\text{O}_2$  cells at 30°C. The initial discharge capacity of samples A, B, C, and D was 107, 137, 140, and 141 mAh/g, respectively. It is evident from the figure that the discharge capacity of sample A increases gradually with cycle number up to the tenth cycle and remains constant at nearly 139 mAh/g, without any loss in capacity even up to 50 cycles. Samples B, C, and D, which were prepared with solvents, delivered higher discharge capacities of 155, 173, and 205 mAh/g, respectively. An increase of discharge capacity with the increase of cycle number has also been observed for all the systems studied.

A similar study has been reported by Kang et al.,<sup>22</sup> where the authors reported the cycling behavior of  $\text{Li}[\text{Li}_{0.2}\text{Ni}_{0.2}\text{Mn}_{0.6}]\text{O}_2$ . According to the authors, the lithium ions are not completely removed during the first charge nor reinserted reversibly in the subsequent cycles. Li ions in the transition metal layer are removed during the initial cycling, and this causes an increase in the discharge capacity.

The corresponding fade in capacity for samples A, B, C, and D are 0.07, 0.41, 0.38, and 0%/cycle, respectively. As shown Fig. 3 and 4, all samples show almost the same charge–discharge behavior, but the discharge capacity of samples prepared with solvent is higher than that of the sample prepared without solvent. It means that the irreversible capacity affects the electrochemical performances, such as discharge capacity and cycle performance. The materials with higher irreversible capacity delivered more discharge capacities with the increase in cycle number.

Furthermore, it is observed from Fig. 4b-d that discharge capacity slightly varies with the nature of the solvent. The discharge capacity of the samples increases in the following order

$$\begin{aligned} \text{Sample D (1-propanol)} &> \text{Sample C (ethanol)} \\ &> \text{Sample B (methanol)} \\ &> \text{Sample A (no solvent)} \end{aligned}$$

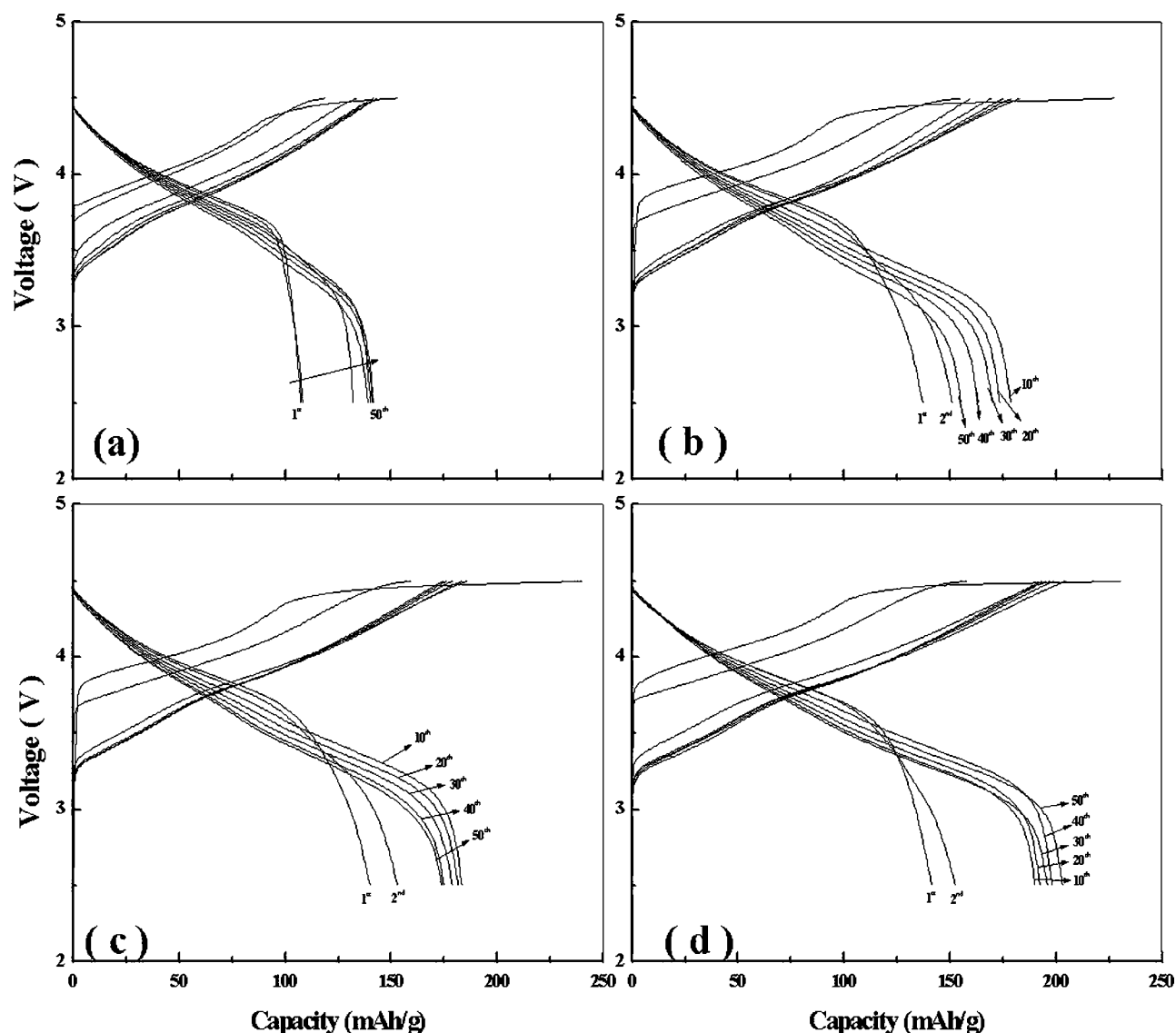
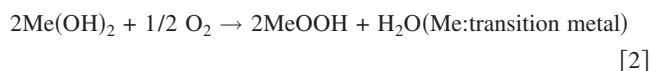


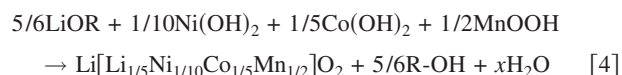
**Figure 3.** Charge–discharge curves of the  $\text{Li}[\text{Li}_{1/5}\text{Ni}_{1/10}\text{Co}_{1/5}\text{Mn}_{1/2}]\text{O}_2$  electrode at a rate of  $0.4 \text{ mA cm}^{-2}$  between 2.5 and 4.5 V (a) without solvent, (b) with methanol, (c) with ethanol, and (d) with n-propanol.

In the solid-state reaction method, solid phase diffusivities take place at higher calcination temperature. The diffusivities can also be enhanced by mechanical mixing of simple ballmilling, as pointed out by Sun et al.<sup>11</sup> The poor solid phase diffusivities of components in solid-state reactions generally lead to the formation of materials with poor stoichiometry, resulting in poor electrochemical characteristics. The diffusivities of the chemical species of the components can be enhanced by the addition of some solvents during the synthesis process. In the present study, three different solvents, namely, methanol, ethanol, or 1-propanol have been used as solvent, and their corresponding reactions are written as follows. The lithium hydroxide reacts with the alcohol in the following way<sup>23-25</sup>



Lithium hydroxide is known to dissolve in alcohol. LiOH dissociates into  $\text{Li}^+$  and  $\text{OH}^-$ , and similarly, ethyl alcohol decomposes

into  $\text{RO}^-$  ( $\text{R:CH}_3\text{CH}_2^-$ ) and  $\text{H}^+$ . During the reaction, the positively charged  $\text{Li}^+$  combines with negatively charged  $\text{OR}^-$  ion and forms LiOR. Accordingly, the  $\text{OH}^-$  ion combines with  $\text{H}^+$  ion, which forms a water molecule. However, this type of reaction is reversible. Forward reaction is much more favorable than the reverse reaction, because LiOH is a stronger base than LiOR. Highly active LiOR is considered to react with MeOOH, followed by the  $\text{H}^+/\text{Li}^+$  ionic exchange reaction, resulting in the formation of  $\text{LiMeO}_2$ . Thus, the formed LiOR participates in the reaction of  $\text{Ni}(\text{OH})_2$ ,  $\text{Co}(\text{OH})_2$ , and  $\text{MnOOH}$  to form  $\text{Li}[\text{Li}_{1/5}\text{Ni}_{1/10}\text{Co}_{1/5}\text{Mn}_{1/2}]\text{O}_2$ . In the present study the following reactions take place and the compound was formed upon calcination at  $960^\circ\text{C}$



The electrochemical behavior varies with the nature of the solvent participating in the chemical reactions. It can be believed that this phenomenon is related to the bond dissociation energy of alcohol. As mentioned in the Introduction section, the dissociation energy, one of the physical properties of the alcohol, plays a vital role

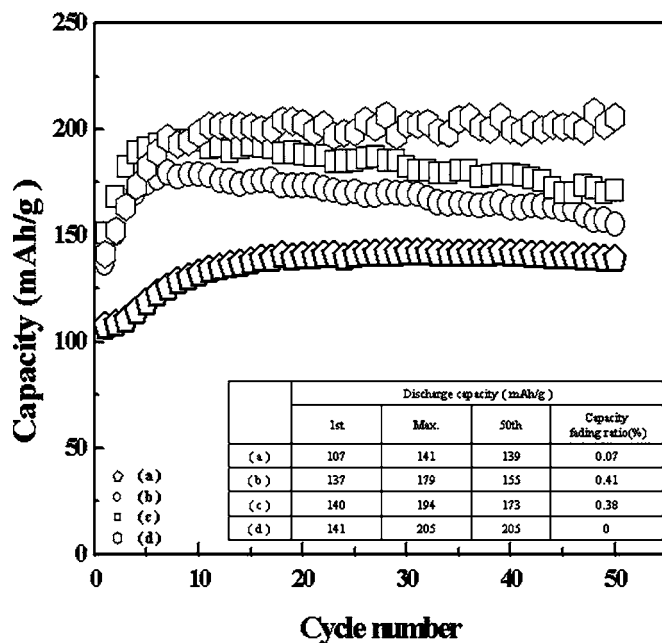


**Figure 4.** Discharge capacity vs. number of cycles for  $\text{Li}[\text{Li}_{1/5}\text{Ni}_{1/10}\text{Co}_{1/5}\text{Mn}_{1/2}]\text{O}_2$  electrode at a rate of  $0.4 \text{ mA cm}^{-2}$  between 2.5 and 4.5 V (a) without solvent, (b) with methanol, (c) with ethanol, and (d) with 1-propanol.

in the structural and electrochemical properties of the compounds formed. The bond dissociation energy of methanol, ethanol, and 1-propanol is 274, 242, and 235 kcal/mol, respectively.<sup>20</sup> The R-OH can be easily dissolved into  $\text{RO}^-$  and  $\text{H}^+$  as the  $\text{R}(\text{CH}_3)_-$  for a longer group chain of alcohol. When the R group has a long chain, the reactivity is decreased due to steric hindrance. The probability of chemical reaction with transition metals increases with the concentration of LiOR. The alcohol, which has the lowest dissociation energy (1-propanol), dissociates easily and facilitates the formation of more transition metals. This results in the formation of compound with good stoichiometry and subsequently exhibits better electrochemical properties. In order to clearly understand this phenomenon, the prepared samples were subjected to FTIR analysis. Figure 5a-d shows the FTIR spectra for  $\text{Li}[\text{Li}_{0.2}\text{Ni}_{0.1}\text{Co}_{0.2}\text{Mn}_{0.5}]\text{O}_2$  prepared with xerogels and dried at  $100^\circ\text{C}$  for 24 h for  $\text{LiOH}\cdot\text{H}_2\text{O}$ ,  $\text{Ni}(\text{OH})_2$ ,  $\text{Co}(\text{OH})_2$ , and  $\text{MnOOH}$  by ballmilling with different solvents.

Figure 5e shows  $\text{LiOH}\cdot\text{H}_2\text{O}$  IR spectra for comparison. The IR spectra of sample A are different from the IR spectra of other samples (B, C, and D). The characteristic peaks at  $400\text{--}600 \text{ cm}^{-1}$  and  $3640 \text{ cm}^{-1}$  are assigned to M-O bending in the higher wavenumber region and the presence of OH groups without bonding formation, respectively.<sup>25</sup> It is quite obvious from Fig. 5 that the IR spectrum of sample A is different from that of the other samples B, C, and D. The peaks which appear at  $3568$  and  $1000 \text{ cm}^{-1}$  in sample A do not appear in other samples, indicating that the unreacted LiOH in the precursor leads to poor stoichiometry of the compound.<sup>26</sup> These results are in accordance with our XRD and Raman spectra data; i.e., the lower intensity of the  $\text{Li}_2\text{MnO}_3$  peak in the XRD pattern and the  $424 \text{ cm}^{-1}$  peak in the Raman spectra. In the case of samples prepared with solvent, the LiOH peaks at  $3568$  and  $1000 \text{ cm}^{-1}$  do not exist, meaning that the addition of solvent during the synthesis process reacts with LiOH, resulting in a material with good stoichiometry. From our XRD refinement data, the lattice parameters,  $a$  and  $c$ , of samples B, C, and D are larger than that of sample A, which means more and more Li ions are inserted into transition metal layers in the compounds B, C, and D. The  $a$  and  $c$  axes increase with an increase in the content of Li ion in the transition metal layers, because the radius of  $\text{Li}^+$  ion ( $\gamma = 0.76 \text{ \AA}$ ) is

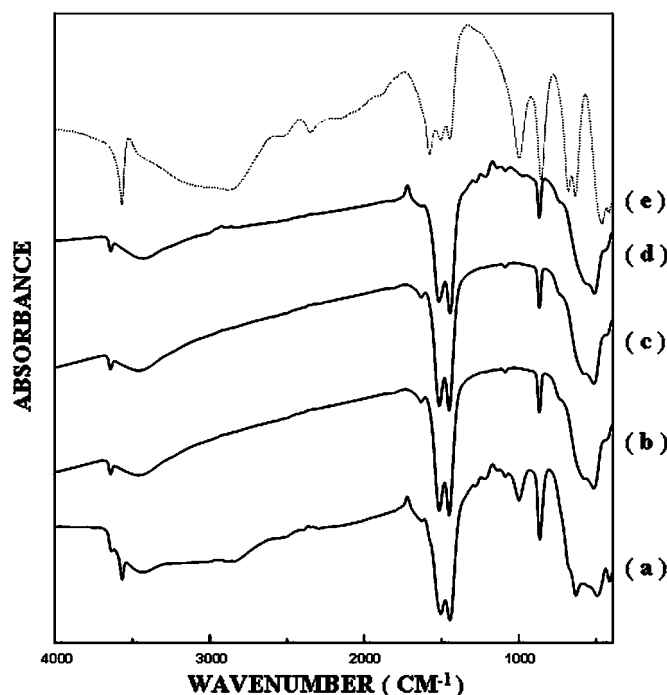


**Figure 5.** FTIR spectra of initial state  $\text{Li}[\text{Li}_{1/5}\text{Ni}_{1/10}\text{Co}_{1/5}\text{Mn}_{1/2}]\text{O}_2$  materials (a) without solvent, (b) with methanol, (c) with ethanol, (d) with 1-propanol, and (e) dashed line is  $\text{LiOH}\cdot\text{H}_2\text{O}$ .

bigger than those of  $\text{Ni}^{2+}$  ( $\gamma = 0.69 \text{ \AA}$ ),  $\text{Co}^{3+}$  ( $\gamma = 0.545 \text{ \AA}$ ),  $\text{Mn}^{4+}$  ( $\gamma = 0.53 \text{ \AA}$ ).<sup>27</sup> This implies that the stoichiometry of the samples prepared with solvent is very close to the standard values of  $a$  and  $c$ . These results are in accordance with those reported for the compound  $\text{Li}[\text{Li}_{0.2}\text{Ni}_{0.1}\text{Co}_{0.2}\text{Mn}_{0.5}]\text{O}_2$  synthesized using the sol-gel method.<sup>12</sup>

## Conclusions

$\text{Li}[\text{Li}_{0.2}\text{Ni}_{0.1}\text{Co}_{0.2}\text{Mn}_{0.5}]\text{O}_2$  was synthesized by solvothermal reaction method with different solvents. As-prepared samples are indexed as a layered manganese oxide structure based on a hexagonal  $\alpha\text{-NaFeO}_2$  structure (space group  $R\bar{3}m$ , 166), except for the superstructure peaks between  $20$  and  $25^\circ$ , which are due to the short-range ordering of Li and Mn in the transition metal layers. The unreacted LiOH compound which exists in sample A during the synthesis process was identified using FTIR analysis. From results, samples B, C, and D exhibited superior electrochemical properties in comparison with sample A. The initial discharge capacities of samples A, B, C, and D were 107, 137, 140, and 141 mAh/g, respectively. The addition of solvents to the precursors during the synthesis process plays an important role in the formation of the compound and subsequently improves the electrochemical properties of the compound.

## Acknowledgment

This work was supported by the Core Technology Development Program of the Ministry of Commerce Industry and Energy (MOCIE).

Chonbuk National University assisted in meeting the publication costs of this article.

## References

1. T. Ohzuku and Y. Makimura, *Chem. Lett.*, **2001**, 744.
2. J. H. Moon, C. S. Yoon, and Y. K. Sun, *J. Electrochem. Soc.*, **150**, A538 (2003).
3. B. J. Hwang, R. Santhanam, and D. G. Liu, *J. Power Sources*, **97-98**, 443 (2001).
4. Z. Lu, L. Y. Beaulieu, R. A. Donabarger, C. L. Thomas, and J. R. Dahn, *J. Electrochem. Soc.*, **149**, A778 (2002).

5. B. Ammundsen and J. Paulsen, *Adv. Mater. (Weinheim, Ger.)*, **13**, 943 (2001).
6. Z. P. Guo, G. X. Wang, H. K. Liu, and S. X. Dou, *Solid State Ionics*, **148**, 359 (2002).
7. J. M. Kim and H. T. Chung, *Electrochim. Acta*, **49**, 937 (2004).
8. J. M. Kim and H. T. Chung, *Electrochim. Acta*, **49**, 3573 (2004).
9. G. Pistoia and R. Rosati, *J. Power Sources*, **58**, 135 (1996).
10. J. Xiao, H. Zhan, and Y. Zhou, *Mater. Lett.*, **58**, 1620 (2004).
11. Y. K. Sun, S. H. Kang, and K. Amine, *Mater. Res. Bull.*, **39**, 943 (2001).
12. K. S. Park, M. H. Cho, S. J. Jin, and K. S. Nahm, *Electrochem. Solid-State Lett.*, **7**, A239 (2004).
13. J. Morales, C. P. Vicente, and J. L. Tirado, *Mater. Res. Bull.*, **25**, 623 (1990).
14. P. G. Bruce, A. R. Armstrong, and R. L. Gitzendanner, *J. Mater. Chem.*, **1**, 193 (1999).
15. C. Julien, S. S. Michael, and S. Ziolkiewicz, *Int. J. Inorg. Mater.*, **1**, 29 (1999).
16. S. S. Shin, Y. K. Sun, and K. Amine, *J. Power Sources*, **112**, 634 (2002).
17. C. Julien, M. A. Camacho-Lopez, T. Mohan, S. Chitra, and P. Kalyani, *Solid State Ionics*, **135**, 241 (2000).
18. C. Julien, *Solid State Ionics*, **136-137**, 887 (2000).
19. C. Julien, *Solid State Ionics*, **157**, 57 (2000).
20. L. G. Wade, *Organic Chemistry*, p. 339, 5/E, Prentice Hall, New York (2003).
21. S.-H. Kang, Y. K. Sun, and K. Amine, *Electrochem. Solid-State Lett.*, **6**(9), A183 (2004).
22. S.-H. Kang, Y. K. Sun, and K. Amine, *Electrochem. Solid-State Lett.*, **6**, A183 (2003).
23. W. T. Jeong and K. S. Lee, *J. Alloys Compd.*, **322**, 205 (2001).
24. Y. Sakurai, H. Arai, and J. Yamaki, *Solid State Ionics*, **113-115**, 29 (1998).
25. D. L. Pavia, G. M. Lampman, and G. S. Kriz, *Introduction to Spectroscopy*, 3rd ed., p. 45, Washington, DC (2001).
26. C.-C. Chang and P. N. Kumta, *J. Power Sources*, **75**, 44 (1998).
27. Z. Lu, D. D. MacNeil, and J. R. Dahn, *Electrochem. Solid-State Lett.*, **4**, A200 (2001).